

Electroproduction of low energy pions from deuterium

G. B. Franklin,* A. M. Bernstein, K. I. Blomqvist, S. A. Dytman,[†] N. Paras,[‡] and M. Pauli[§]

Physics Department and Laboratory for Nuclear Science, Massachusetts Institute of Technology, Cambridge, Massachusetts 02139

J. LeRose,** K. Min, D. Rowley,^{††} B. O. Sapp,^{‡‡} P. Stoler, E. J. Winhold, and P. F. Yergin

Physics Department, Rensselaer Polytechnic Institute, Troy, New York 12181

(Received 11 April 1984)

The inclusive electroproduction of 30 MeV π^+ and π^- mesons has been observed at a laboratory angle of 90° for electron energies from 185 MeV (the kinematic threshold) to 235 MeV. Measurements of the yield were performed and double differential cross sections for photoproduction were obtained using virtual-photon theory. A significant discrepancy between experiment and distorted-wave impulse approximation calculations was found. This is particularly surprising since these calculations agree with the total cross sections for the ${}^2\text{H}(\gamma, \pi^+)nn$ reaction from threshold to 20 MeV above threshold.

I. INTRODUCTION

The elementary photopion process on the proton, $\gamma + p \rightarrow \pi^+ + n$, has been extensively studied experimentally,¹ and is well understood theoretically,²⁻⁴ particularly for energies from threshold through the Δ (1236 MeV) resonance. Photopion calculations for complex nuclei make use of this elementary amplitude by use of the impulse approximation (see, e.g., Ref. 5). It is therefore of interest to make a systematic experimental study of the validity of this approach. The deuteron represents the simplest test because of its low density and because of its relatively well-known structure. In the past few years, the total cross section for the ${}^2\text{H}(\gamma, \pi^+)nn$ reaction in the region of 1–20 MeV above threshold has been carefully measured,⁶ relative to the elementary proton cross section, and found to be in good agreement with impulse approximation calculations.^{7,8} In order to extend this test, we have measured the double differential cross section for the electroproduction of 30 MeV pions from deuterium. This provides stricter control of the kinematical variables than the total cross section measurements, and as a consequence it is more sensitive to the details in the calculation such as the final state interactions. The pion energy of 30 MeV, somewhat larger than in the total cross section measurements, was chosen to be well below the delta region so that the final state π -N interaction would be small through most of the kinematic region explored.^{8,9}

Valuable data were also obtained from the ${}^2\text{H}(\gamma, p\pi^-)p$ coincidence experiment performed at Saclay.⁸ The Saclay experiment chose kinematics that emphasize the production of the Δ resonance, i.e., strong final state interactions. Data were also taken with quasifree kinematics that verifies the accuracy of the basic distorted-wave impulse approximation (DWIA) model⁸ in the energy region explored in the Saclay experiment. The calculations used in this paper are based on the same model.

II. EXPERIMENTAL RESULTS

Our experiment was performed on the low energy pion spectrometer at the Bates Linear Accelerator.¹⁰ The electron beam passed through a deuterium gas target pressurized to 25 atm (Ref. 11) and cooled with liquid nitrogen. The QD spectrometer was fixed at 90° (lab) and set to accept 25–33 MeV pions for all data runs. The pion momentum was determined with a multiwire proportional chamber that measured the position along the bend direction of the focal plane. Pions were distinguished from other particles (mainly electrons or positrons) by measuring the energy deposited in an array of three scintillators and the light output of a Lucite Čerenkov detector. The total energy resolution for the experiment was about 2.2 MeV (FWHM). Data for π^+ and π^- production were collected at 13 electron beam energies ranging from 187 to 230 MeV. At the lowest beam energies, the spectrometer's energy acceptance included a region in which pion production from deuterium was prohibited by kinematics. This provided a test of the particle identification and background reduction procedures.

The background situation was somewhat better than that encountered in Ref. 10 because the cross sections are higher and the shielding was improved. A tungsten collimator 2 cm thick effectively blocked the spectrometer's view of the front and back target walls. Data runs with an empty target produced pion count rates of only a few percent of those measured with a full target. The number of electrons surviving all cuts was estimated to be $\sim 10\%$ of the pions at the kinematic threshold, decreasing to $\sim 3\%$ at the highest electron energies. A Monte Carlo calculation¹¹ determined the muon background to be only a few percent.

A single target vessel was used for all data runs so that conditions for deuterium, hydrogen normalization (discussed in the following), and empty target runs were

essentially identical. The temperature and pressure were monitored continuously and data were taken only when conditions were stable. Microscopic heating effects were checked by varying the peak current of the electron beam. Yields varied by about 2% (consistent with expected statistical variations) for 50% changes in the peak current.

For a fixed N-N excitation energy, the yield was found to be a slowly varying function of the pion energy and could then be considered to be a constant over the energy acceptance of our spectrometer. Thus the individual spectra could be combined without loss of information into a single yield distribution for 30 MeV pions as a function of incident electron energy. This procedure has been carefully checked.¹¹

To obtain an absolute normalization, the deuterium gas was replaced with hydrogen and the differential cross section for the reaction $p(\gamma, \pi^+)n$ was measured with a 230 MeV electron beam. These elementary production data were then normalized to the calculations of Blomqvist and Laget,⁴ which give a value of $8.5 \mu\text{b}/\text{sr}$ for the production of 30 MeV pions at 90° lab angle (consistent with previous experimental data¹). This technique minimizes experimental uncertainties in target thickness, detector efficiencies, solid angle, etc. The systematic uncertainties in target thickness, beam intensities, etc., were estimated to be 11%. This was combined with a 10% uncertainty in the theoretical hydrogen cross section to give a total estimated systematic error of 15% in the absolute normalization of the experimental results. This error is not included in any of the figures discussed in the following.

The normalization procedure already described was used in the computations of yields, but was verified in two ways. An absolute determination of the differential cross section for $p(\gamma, \pi^+)n$ at 192 MeV photon energy was made from our normalization data. The spectrometer solid angle was measured with elastic electron scattering from ^{27}Al and the gas target thickness was calculated from the measured temperature and pressure. The result is 5% less than the Blomqvist-Laget value with an estimated error of $\pm 20\%$. To prove that the gas target geometry suppressed background particles, hydrogen data were also taken with a solid target (CH_2). After subtracting the yield from carbon obtained in a separate measurement, the cross section was found to be 3% larger than the Blomqvist-Laget value.

The raw data include pions from both electroproduction and photoproduction processes. The number of photoproduction events was calculated independently¹²⁻¹⁴ and subtracted from the total. Since about 30% of the events were due to photoproduction, the additional error introduced in this subtraction was only a few percent. The entire procedure for obtaining yield values is described in greater detail in Ref. 14. The electroproduction yields for this experiment are shown in Fig. 1.

The electroproduction yields have been converted to photoproduction cross sections through the use of virtual photon theory. This common method of interpretation views the interaction of the electron with the nucleus as the exchange of a single virtual photon. If the cross section for a virtual photon is the same as that for a real photon, the electroproduction yields at beam energy E_0

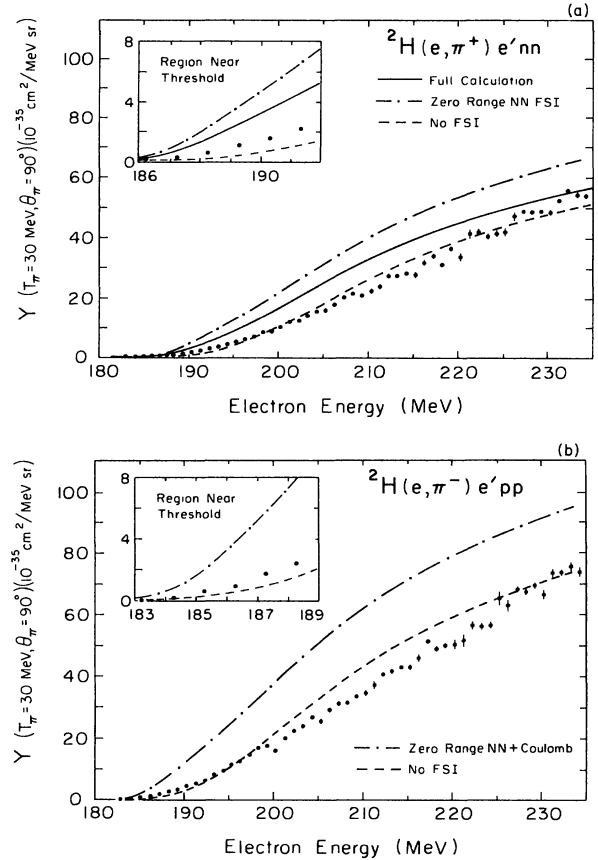


FIG. 1. Electroproduction yield data in the laboratory system for this experiment. The yield is measured for 30 MeV pions detected at 90° lab angle as a function of incident electron energy. The π^+ data are shown in part (a) and the π^- data in part (b). An insert in each figure shows an expanded view of the data and calculations near threshold. Only relative errors are shown; the estimated absolute error is $\pm 15\%$. In each part, the dashed line gives the results of calculations with no FSI. In part (a), the dot-dash and solid lines show calculations with nn FSI for a zero range force and the complete Yamaguchi interaction, respectively. In part (b), the dot-dash curve is a calculation with zero range strong interaction and full Coulomb interaction for the outgoing pp pair.

can be related to a sum of photoproduction cross sections at photon energies k , through the virtual photon spectrum N_e ,

$$Y(E_0, T_\pi) = \int_0^{E_0 - m_c} N_e(E_0, k) \frac{d^2\sigma}{d\Omega dT_\pi}(k, T_\pi) \frac{dk}{k}. \quad (1)$$

The spectrum of Dalitz and Yennie¹⁵ has been in common use since the late 1950's and we use it here. Very recently, theoretical work by Tiator and Wright¹⁶ showed the Dalitz-Yennie virtual photon spectrum to be an average of about 5% larger than their more exact calculation for π^+ production from hydrogen within a few MeV of the end point with approximately the same kinematics as this experiment. The ^1H and ^{12}C data¹⁷ taken at Mainz support the Tiator-Wright calculation. We have verified that the

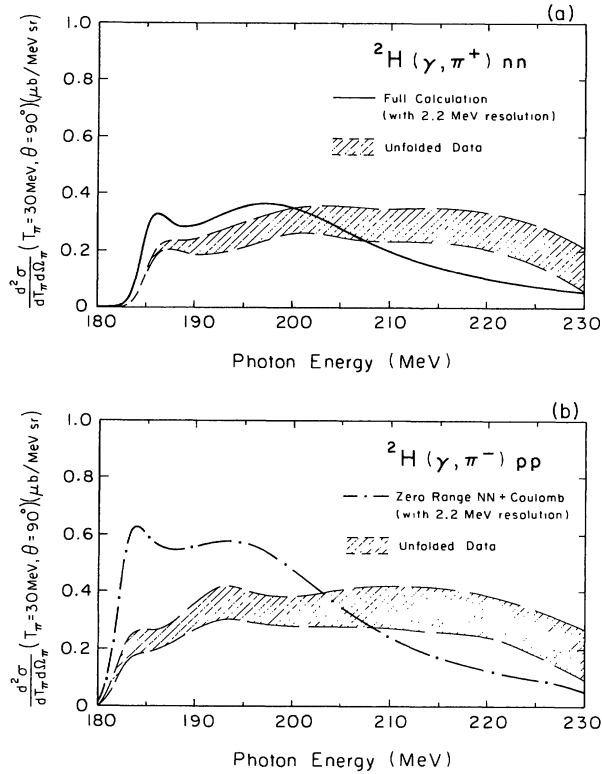


FIG. 2. The photoproduction cross sections determined from this experiment are plotted for π^+ and π^- as a function of photon energy in the laboratory. The crosshatched band defines the region in which the cross section curve will most likely (within 1 standard deviation) be. Absolute normalization errors (estimated to be $\pm 15\%$) are not shown. The cross section calculations corresponding to the most accurate yield calculations in Fig. 1 are shown with the same meaning for symbols. The calculations have had the experimental resolution folded in.

Tiator-Wright spectrum would not change any of the conclusions of this work.

Equation (1) must be inverted to derive photoproduction cross sections. This was done with a least structure unfolding method.¹¹ The unfolded photoproduction cross sections are shown (with statistical errors only) in Fig. 2. Because the energy resolution of the apparatus was ~ 2.2 MeV, it is unlikely that the sharp structure predicted at threshold in the theory (see Fig. 4) could be unfolded. Therefore, the data were unfolded with the resolution left in and the calculations were folded with the experimental resolution to give the most accurate comparison of data with the calculation.

III. COMPARISON WITH THEORY

The data were compared to a photoproduction DWIA calculation¹¹ based on the work of Dressler *et al.*¹⁸ This calculation uses the amplitudes of Blomqvist and Laget⁴ to describe the elementary production mechanism. The deuteron wave function and the final state N-N interaction were fixed by using an *S*-wave Yamaguchi¹⁹ separable potential to describe the N-N interaction. The potential parameters were fit to the deuteron's binding ener-

gy and the N-N scattering length and effective range. No pion-nucleon final state interactions were included in the calculation.

A diagram of the kinematic variables relevant to this calculation for ${}^2\text{H}(\gamma, \pi)\text{NN}$ is shown in Fig. 3(a). In the center-of-mass system, a photon of momentum k is absorbed on a single nucleon and produces a pion of momentum q . The relative momentum of the two nucleons is \vec{p}' in the initial state and \vec{p}_f in the final state. Figures 3(b) and 3(c) show the distributions of some of the variables for 30 MeV pions produced at 90° in the laboratory. The struck nucleon receives a momentum transfer $\vec{Q} = \frac{1}{2}(\vec{k} - \vec{q})$, as seen by the center of mass of the NN system. Although \vec{Q} is small for all the data of this measurement, the relative momentum of the two final nucleons (\vec{p}_f) rises dramatically as k increases. For a fixed pion energy and angle, the magnitude (but not the direction) of \vec{p}_f is fixed by the photon energy.

If there is no N-N final state interaction, the final momentum of the struck nucleon $\vec{p}_f = \vec{p}' + \vec{Q}$. Since the final state nucleons are not detected, the calculation of the cross section involves an integral over the direction of the vector \vec{p}_f . For a plane wave final state system, this integral maps directly to an integral over the struck nucleon's momentum \vec{p}' . In this case, the integral covers the range $|p_f - Q| < p' < |p_f + Q|$. This range is illustrated in Fig. 3(c). If this region is compared to the deuteron wave function in Fig. 3(d), we see that for $k - k_{\text{th}} \gg 30$ MeV, production of a 30 MeV pion involves the higher momentum components of the deuteron wave function and one expects the cross section to be small and decreasing for large photon energies. Although this argument applies only if there are no final state interactions (FSI's), calculations show it to be true with FSI's as well.²⁰

Since the relative N-N momentum is small near $k = k_{\text{th}}$, we can expect significant effects from the strong *S*-wave nucleon-nucleon interaction. Also, the repulsive Coulomb force between the outgoing protons may be expected to suppress the production of negatively charged pions.

The photoproduction calculation already described was compared with the π^+ electroproduction data by folding it with the virtual photon flux and the spectrometer's resolution function. The results are shown in Fig. 1(a) with three treatments of the final state N-N interaction. The solid line shows the "full" calculation which uses Yamaguchi wave functions, the dash-dot line shows a calculation using a zero-range N-N interaction, and the dashed line is a plane wave calculation. All three neglect contributions from π -N rescattering. An insert in the same figure shows an expanded view of the region near threshold.

A similar calculation was performed for the ${}^2\text{H}(e, \pi^-)\text{ppe}'$ data. This required the substitution of the π^- elementary production amplitudes and treatment of the Coulomb final state interactions. The π -p Coulomb interaction was estimated with the Sommerfeld suppression factor to be only a 3% correction and therefore was neglected. However, the p-p Coulomb force gives large effects, particularly when the kinematics require the two protons to have small relative momenta. Thus the p-p

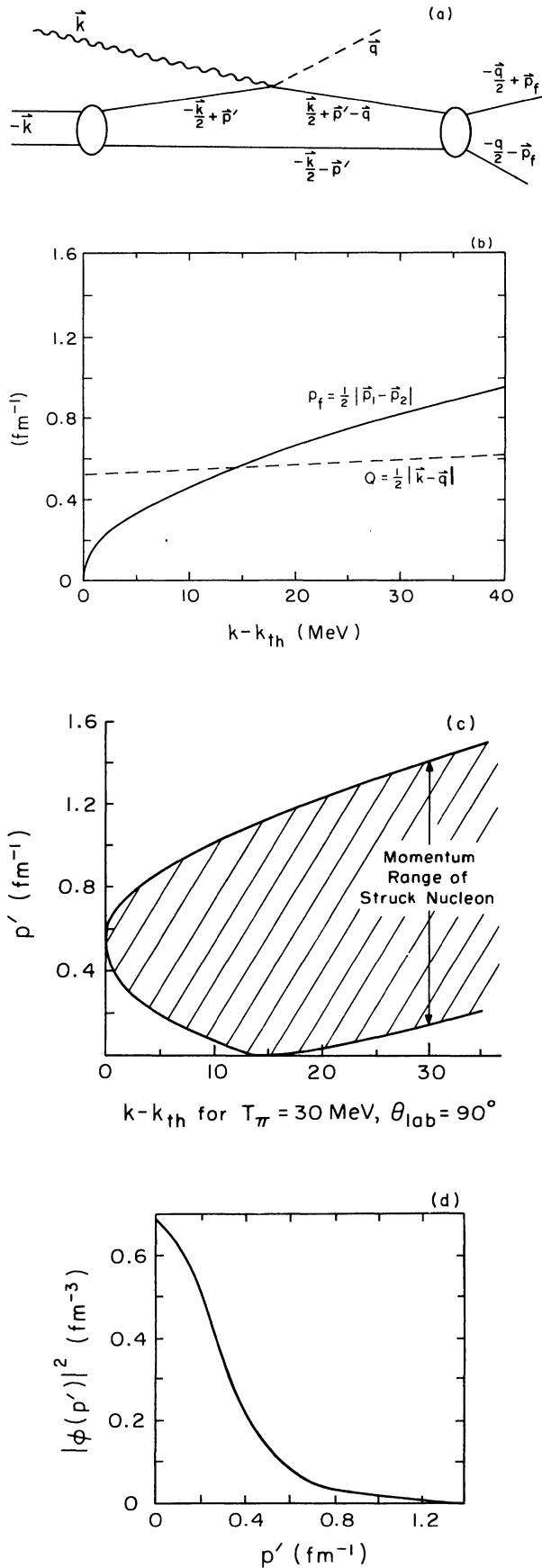


FIG. 3. Kinematics for the photoproduction calculations of this paper. Part (a) shows the diagram that is calculated with the momentum of each particle in the center of mass system. Part (b) shows the momentum transfer to the struck nucleon (Q) and the relative momenta of the two nucleons in the final state (P_f) as a function of the photon momentum above threshold. In part (c), the kinematically allowed momenta for the struck nucleon for the calculation with no FSI are plotted as a function of the photon energy above threshold. Part (d) shows the deuteron wave function used.

Coulomb force counteracts the strong N-N S -wave attraction and reduces the spike in the cross section at the minimum photon energy.

The effect of the combined nuclear and Coulomb p - p final state interactions was calculated using a numerical solution to describe the outgoing p - p wave function for a zero range N-N interaction. The resulting photoproduction cross sections were then folded with the virtual photon flux and the spectrometer's resolution function to give the electroproduction yield shown in Fig. 1(b). The results with no final state interaction are also shown.

It can be seen that the calculations for both π^+ and π^- production predict yields which have a larger slope than the data for electron energies up to 210 MeV, indicating theoretical cross sections which are larger than those implied by the experimental yields. Around 210 MeV, the experimental yields increase faster than the theoretical curves, indicating that the theoretical cross sections are too small in this region.

The data can also be compared to the theoretical cross sections by unfolding the experimental yields [see Eq. (1)]. Figure 2(a) shows the unfolded experimental cross sections for π^+ production as the crosshatched area. The errors represented are statistical only. For the best comparison with the data, the calculations shown in Fig. 2 have been folded with the experimental resolution (FWHM = 2.2 MeV). The theoretical calculations without this effect are shown in Fig. 4(a). In the first 5 MeV above the minimum photon energy, the plane wave calculation is below the data. Inclusion of the N-N final state interaction with Yamaguchi wave functions enhances the cross section, but the results lie well above the data. Final state interactions have a small effect for photon energies more than 10 MeV above threshold. The results of a zero range N-N interaction calculation are shown to give an indication of the sensitivity to the range of the nuclear force.

Figures 2(b) and 4(b) show the unfolded π^- data and the results of the calculations discussed earlier. The π^- calculation in Fig. 2(b) (using a zero range force and Coulomb wave functions) has even larger discrepancies with respect to the data than is seen in the π^+ case. This can also be seen in Fig. 5, which shows the π^-/π^+ cross section ratios. The solid line represents the π^- calculation divided by the separable potential π^+ calculation. A better agreement with data is obtained when the ratio is calculated in a more self-consistent manner using a zero range N-N force in both the π^- and π^+ calculations. This effect may be fortuitous since the Coulomb suppression of the short range p - p wave functions is expected to

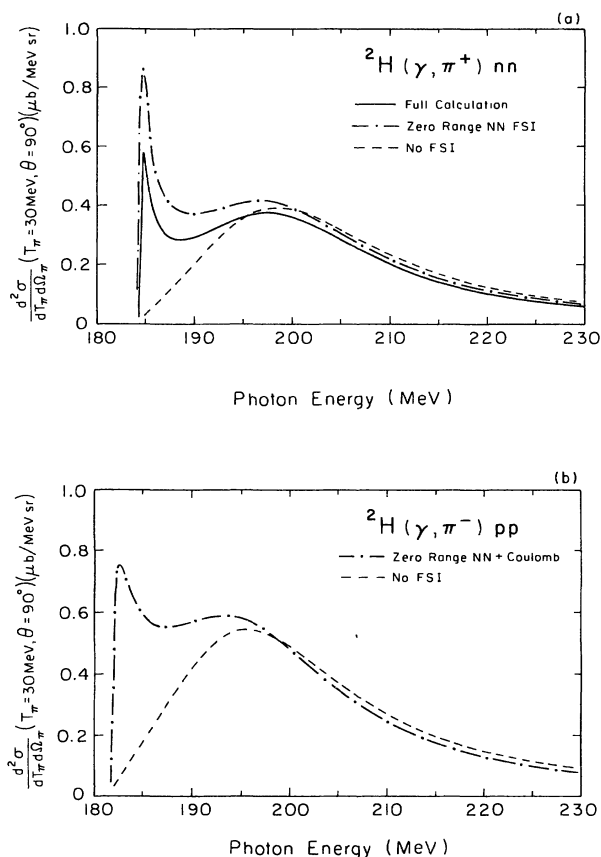


FIG. 4. The results of various cross section calculations are shown with no resolution effects included. The curves are labeled with the same symbols as in Fig. 1.

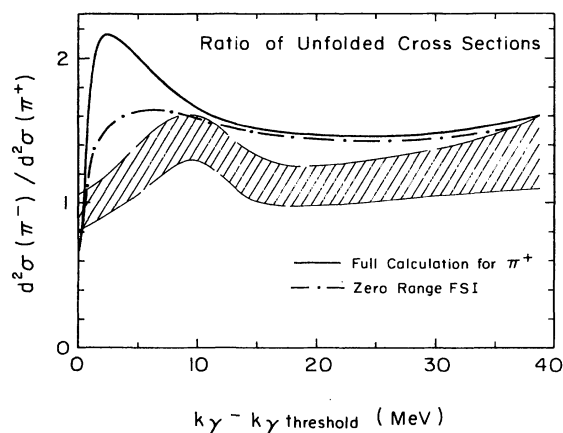


FIG. 5. The ratio of π^- to π^+ differential cross sections as a function of photon energy. Both calculations use the π^- calculation with a numerical Coulomb wave function [dot-dash line in Figs. 1(b) and 2(b)]. The solid line uses the full π^+ calculation [solid line in Figs. 1(a) and 2(a)] and the dashed line uses the zero range π^+ calculation [dot-dash line in Figs. 1(a) and 2(a)].

make the π^- calculation less sensitive to the zero range force approximation than the π^+ calculation.

Not only are the calculations in Fig. 2 too high near threshold, but they are too low at larger energies. This discrepancy may not be as significant because the unfolded cross section at these higher energies is particularly sensitive to statistical and systematic errors in the yield function. However, the nonzero slopes of the yields from 210 to 235 MeV for both π^- and π^+ production in Fig. 1 clearly indicate a finite cross section in this interval.

IV. CONCLUSIONS

The energy dependence of experimental yields and unfolded cross sections for ${}^2\text{H}(\gamma, \pi^\pm)$ for 90° lab pion angle have been presented. The yields are certainly more accurate because they are directly related to the raw data. The cross sections have unfolding errors that clearly grow with photon energy, but are very difficult to estimate; we choose to present only statistical errors. On the other hand, cross sections are much easier to interpret and are more directly related to the relevant physics. We have tried to show that an analysis from either form of data would give similar conclusions.

We have seen a theoretical model which has been successful in describing photoproduction total cross sections for π^+ production from deuterium near threshold fail to produce the same agreement with the data from this experiment. There is a large disagreement near the kinematic minimum where final state N-N interactions are important, and a lesser problem above the quasifree peak where the calculations predict a sharper decline than is exhibited by the data. Since the previous successes of the impulse approximation have been used to justify this form of calculation in other (γ, π) reactions, it is important to determine whether this experiment represents a true failure of the impulse approximation or if the disagreements are only the results of the other approximations used in this particular calculation. To this end, a more complete calculation is in order. A better deuteron wave function, with inclusion of the D state and associated angular momentum algebra, should be used. Since the elementary production amplitude is a slowly varying function of the struck nucleon momentum, the amplitude has been factored out of the integral over the struck nucleon momentum. While this decreases the amount of numerical computation, it may also add to the error.

The calculations discussed here have neglected the final state π interaction. Calculations similar to the ones already described but incorporating both the N-N and π -N final state interaction were recently performed for the kinematics of this experiment by Laget,^{8,20} with results that are within a few percent of those neglecting the π -N final state interaction which we presented. The same model has been applied to recent Saclay inclusive pion photoproduction data for deuterium in the Δ region.⁸ The agreement of the calculations with this new data is good on the quasielastic peak, but they note a discrepancy similar to the one reported here when the pion energy is at the kinematic limit. Although this discrepancy is not as large as the one reported in this paper, these newer data are also not as sensitive to the NN interaction.

ACKNOWLEDGMENTS

The authors are grateful to the Bates Linac staff for work on the gas target. We are also indebted to J. O'Connell and J. M. Laget for their invaluable discussion

of the theoretical aspects of the paper and for the use of their computer codes. This work was supported by Grant DE-AC02-76-ER0-3069 of the Department of Energy and by Grants PHY77-09408 and PHY80-06954 of the National Science Foundation.

*Present address: Department of Physics, Carnegie-Mellon University, Pittsburgh, PA 15213.

†Present address: Department of Physics, University of Pittsburgh, Pittsburgh, PA 15260.

‡Present address: Bell Telephone Labs, Murray Hill, NJ 07974.

§Present address: General Research Corporation, 7655 Old Springhouse Road, Westgate Research Park, McLean, VA 22102.

**Present address: Department of Physics, Louisiana State University, Baton Rouge, LA 70803.

††Present address: Lawrence Livermore Laboratory, Livermore, CA 94550.

‡‡Present address: 46 Cresthill Road, Brighton, MA 02135.

¹D. Menze, W. Pfeil, and R. Wilcke, ZAED Physics Data 7-1 (1977).

²G. F. Chew, M. L. Goldberger, F. E. Low, and Y. Nambu, Phys. Rev. **106**, 1345 (1957); **106**, 1337 (1957).

³F. A. Berends, A. Donnachie, and D. L. Weaver, Nucl. Phys. **B4**, 1 (1967); **B4**, 54 (1967); D. Schweda *et al.*, Z. Phys. **202**, 452 (1967); **221**, 71 (1969).

⁴I. Blomqvist and J. M. Laget, Nucl. Phys. **A280**, 405 (1977).

⁵M. K. Singham and F. Tabakin, Ann. Phys. (N.Y.) **135**, 71

(1981).

⁶E. C. Booth *et al.*, Phys. Lett. **66B**, 236 (1977); Phys. Rev. C **20**, 1217 (1979); G. Audit *et al.*, *ibid.* **16**, 1517 (1977).

⁷J. M. Laget, Nucl. Phys. **A296**, 388 (1978).

⁸J. M. Laget, Phys. Rep. **69**, 1 (1981).

⁹B. H. Bransden and R. G. Moorhouse, *The Pion-Nucleon System* (Princeton University, Princeton, N.J., 1973).

¹⁰N. Paras *et al.*, Nucl. Instrum. Methods **167**, 215 (1979).

¹¹G. Franklin, Ph.D. thesis, MIT, 1980 (unpublished).

¹²J. L. Matthews and R. O. Owens, Nucl. Instrum. Methods **111**, 157 (1973).

¹³R. J. Jabbur and R. H. Pratt, Phys. Rev. **129**, 184 (1961).

¹⁴M. Pauli, Ph.D. thesis, MIT, 1981 (unpublished).

¹⁵R. H. Dalitz and D. R. Yennie, Phys. Rev. **105**, 1598 (1957); W. C. Barber and T. Wiedling, Nucl. Phys. **18**, 575 (1960).

¹⁶L. Tiator and L. E. Wright, Nucl. Phys. **A379**, 407 (1982).

¹⁷C. Schmitt *et al.*, Nucl. Phys. **A392**, 345 (1983).

¹⁸E. T. Dressler, W. M. MacDonald, and J. S. O'Connell, Phys. Rev. C **20**, 267 (1979).

¹⁹Y. Yamaguchi, Phys. Rev. **95**, 1628 (1954).

²⁰J. M. Laget (private communication).